

※ 考生請注意：本試題不可使用計算機。請於答案卷(卡)作答，於本試題紙上作答者，不予計分。

一. 問答題：(每題 10 分，共 20 分)

1. 請敘述您報考臨床醫學研究所的主要動機為何？這樣對您將來的醫學生涯規劃有何影響？
2. 試舉一臨床例子說明何謂標靶治療(targeted therapy)?同時說明其優缺點，及提出可行的方式以改善，增加其作用及避免標靶藥物產生的副作用。

二. 簡答題：(每題 6 分，共 30 分)

1. 請敘述細胞死亡(cell death)之種類及其特性
2. 就您所知，請例舉臨床癌症一例子解釋癌症之發生(carcinogenesis)
3. 何謂 induced pluripotent stem cells (iPSCs)? 臨床上有何可能之使用?試舉例解釋之。
4. 下腹部疼痛(low abdominal pain)之鑑別診斷。
5. 何謂 Next Generation Sequence (NGS)?對於現代醫學有何應用及影響?試舉例說明之。

三. 申論題：(請選五題申論，每題 10 分，共 50 分)

1. 安寧緩和醫療是針對不可治癒的末期病患提供全人、全家、全隊、全程、全社區的「五全」照顧，這也是當前世界各國公認為對疾病末期病人醫療照顧模式的最佳選擇。請就生活品質，提出一個客觀評估的研究，說明安寧醫療的重要。
2. 臺灣從 1984 年 7 月 1 日全面施行新生兒 B 型肝炎疫苗接種，希望年輕一代，人人體內都有 B 肝表面抗體，對 B 肝病毒具有免疫力(抵抗力)。請以公衛預防醫學的角度，來談這政策的影響。
3. 許多醫院都引進高科技的「Proton therapy」或「Robot-assisted surgery」來嘉惠病人，就你的了解，請簡述之。
4. 以下為一新聞的標題：「Precision medicine can be a clinical reality: Use of HLA-B*58:01 genotyping to prevent allopurinol-induced severe cutaneous adverse reactions in Taiwan」。請你舉出其他的例子說明，precision medicine 在臨床運用。
5. 單株抗體在癌症治療已廣泛運用，但還有其他疾病，臨床上也在使用，請舉出 3 例說明之。(提示：免疫、心血管、氣喘、骨質疏鬆、ulcerative colitis 等疾病)。
6. 火，是文明的象徵，開啟人類新的紀元，但火的技術衍生出對自然資源造成急劇消耗，且對自然環境產生污染。同樣的，奈米科技為人類帶來新的美好，但會產生什麼災難嗎？請就你的了解說明「奈米醫學」的一體兩面。
7. 糖尿病患者，養成持續且規律的運動習慣，可幫助血糖的控制。請就 insulin resistance 的概念來闡述。
8. 請簡述流感併發重症 (Severe Complicated Influenza) 的定義、致病機轉及治療原則。
9. 請簡述 Stem Cells 及 Cancer Stem Cells 有哪些特性，它們目前及將來在臨床醫學的運用。
10. Functional MR imaging of tumor angiogenesis predicts outcome of patients with acute myeloid leukemia. Shih TT et al., *Leukemia* 2006;20:357-362..... 該研究為 Functional imaging 在醫學上的應用。請說明 Functional imaging 定義，並舉例說明。(本篇文章參考:第 2 頁至第 5 頁)

Functional MR imaging of tumor angiogenesis predicts outcome of patients with acute myeloid leukemia

Leukemia (2006) 20, 357–362. doi:10.1038/sj.leu.2404066; published online 15 December 2005

It is well recognized that angiogenesis plays an important role in tumor development, progression and metastasis,¹ and also

with active disease in comparison to normal controls or patients in remission.³ However, MVD can only be measured in the very limited area of the bone marrow needle biopsy specimen and is unable to assess global or *in vivo* tumor angiogenesis. The functional status of the blood vessel (e.g. permeability) could not be determined by MVD. Moreover, MVD cannot determine whether a particular therapeutic compound is primarily directed against the angiogenic response of the tumor.⁴ Thus, the needs of a rapid and effective angiodiagnostic imaging to establish antiangiogenic drug dosage or monitor treatment response is important.

Dynamic contrast-enhanced magnetic resonance imaging (dMRI) techniques allow quantification of blood perfusion and also provide information on the functional status of the blood vessels, including blood flow and vascular permeability.⁵ Increased angiogenesis of the bone marrow was detected by dMRI in patients with multiple myeloma and myelodysplastic syndrome.⁶ Tumor angiogenesis imaging assessment in AML patients has not been reported. In this study, we developed an algorithm for dMRI to evaluate and visualize the *in vivo* tumor angiogenesis in patients with newly diagnosed acute myeloid leukemia (AML) and correlated it with clinical outcome.

From December 2001 to April 2003, a total of 17 adult patients with newly diagnosed AML were enrolled. The median age was 37 years (range: 18–74 years). In total, 17 age and gender matched normal volunteers were used as control. Every patient received bone marrow examination (aspiration/core biopsy) from the iliac crest. Diagnosis and classification of AML were made according to the French-American-British (FAB) criteria. All patients received dMRI (median of 1 day, range: 0–2 days) before induction chemotherapy of idarubicin 12 mg/m² per day on days 1–3 and cytosine arabinoside (Ara-C) 100 mg/m² per day on days 1–7. After complete remission (CR) was achieved, the patients received consolidation chemotherapy with either the same regimen as that of induction chemotherapy or high-dose Ara-C. All patients were followed up to March 2005. A total of 15 patients (88%) obtained a CR and eight (47%) remained disease free.

MR imaging of the spine was performed in every AML patient and normal control with a 1.5-T superconducting system (Magnetom Vision Plus; Siemens, Erlangen, Germany). A phase-array spine-coil was used and dMRI study was performed (section thickness, 10 mm; field of view, 28 cm) at the mid-sagittal plane of the vertebral bodies from T11 through the sacrum as described in our previously studies.⁷ An injection of 0.1 mmol/kg body weight of gadopentetate dimeglumine (Magnevist; Schering, Berlin, Germany) was administered by the power injector through a 21-gauge intravenous catheter in the right antecubital vein. A constant injection rate of 2.0 ml/s was used. Dynamic scanning was started when the injection of the contrast material commenced. The pulse sequence for the dynamic scanning used was a turbo fast low-grade shot gradient-echo sequence (8.5/4.0; prepulse inversion time, 160 ms; flip angle, 10°; acquisition matrix, 72 × 128). In total, 100 dynamic images were obtained at one frame per second for 100 s in each subject.

Signal intensity values were measured in an operator-defined region of interests (ROIs) by the radiologist, covering the entire vertebral body. The signal intensity values derived from the ROI were then plotted against time to obtain a time-signal intensity curve (Figure 1a). The baseline value for signal intensity (SI_{base}) on a time-signal intensity curve was defined as the mean signal intensity from the first three images. The maximum signal intensity (SI_{max}) was defined as the maximum value of the rapidly rising part or first pass of the time-signal intensity curve.

correlates with clinical outcome in cancer patients with melanoma, prostate cancer, breast cancer, and recently in leukemia and lymphoma.²

Microvessel density (MVD) shown by immunohistochemical staining with anti-CD31 is a 'gold standard' for the detection of angiogenesis in tumor tissue. MVD is increased in AML patients

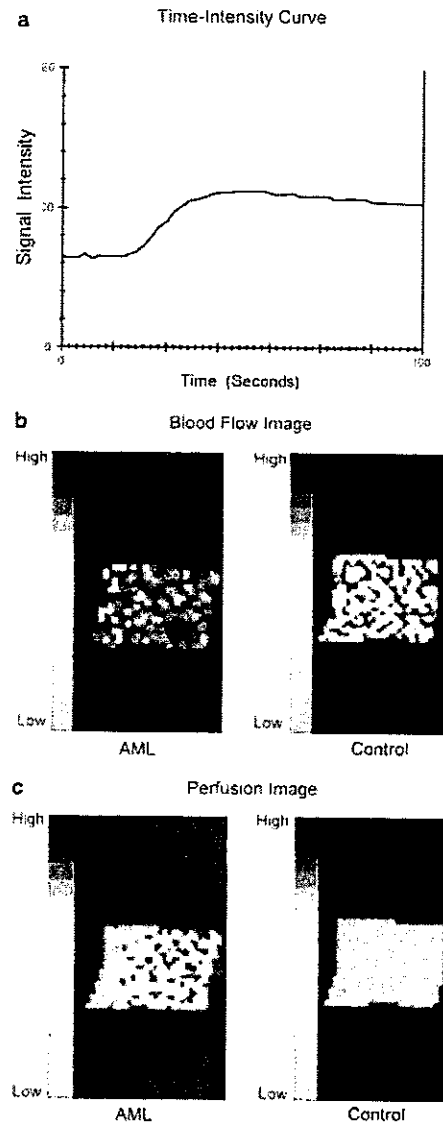


Figure 1 Time-intensity curve and color-coded bone marrow blood flow and perfusion images of AML patient and normal control. (a) Time-intensity curve from the lumbar vertebral dMRI. (b, c) Color-coded bone marrow blood flow and tissue perfusion images of AML patient and normal control. The blood flow image was the mapping for initial enhancement slope of one segment of vertebral body at early increment phase. The tissue perfusion image was the mapping for peak enhancement ratio at the mid-equilibrium phase. Obvious difference could be identified between them by the visualization of angiogenesis map.

After the peak, which usually occurred about 40 s after the start of injection, the time-signal intensity curve entered an equilibrium phase that lasted about 30 s.⁷ For the semiquantitative analysis, the peak enhancement ratio (peak) was calculated for each ROI as $(SI_{\text{max}} - SI_{\text{base}}) / SI_{\text{base}}$ and initial

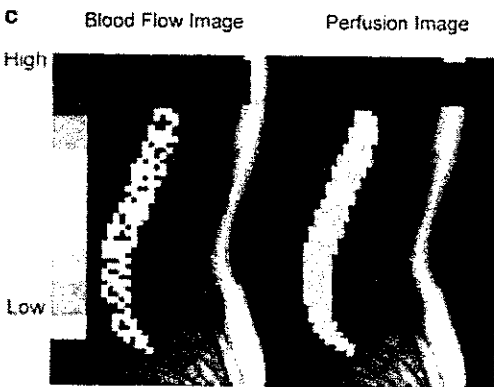
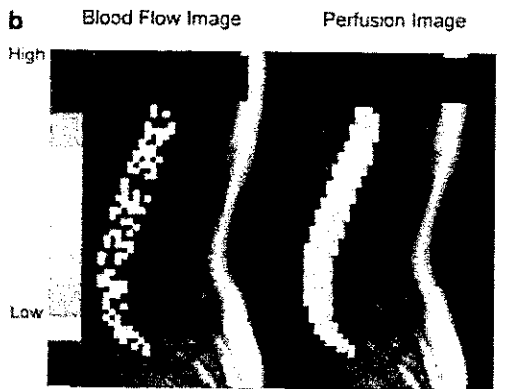
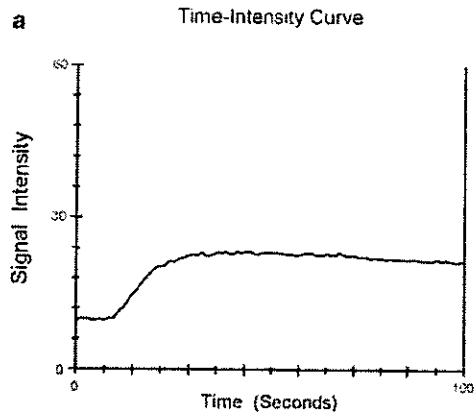


Figure 2 Dynamic magnetic resonance imaging study in a 37-year-old female with newly diagnosed AML. She remained disease free after chemotherapy. (a) Time-intensity curve from the vertebral dMRI showed slow, uprising increment during the first-pass, which indicated low angiogenesis of the bone marrow. (b) Color-coded blood flow (slope) and perfusion (peak) images at early increment phase of the dynamic scanning. (c) Color-coded blood flow (slope) and perfusion (peak) images at mid-equilibrium phase of the dynamic scanning. (b,c) The angiogenesis map of the vertebral bone marrow was automatically displayed from 0 to 100s of the dMRI: the red color represented high angiogenesis, yellow as intermediate and green color as low angiogenesis, shown in the color-coding bar chart.

maximum enhancement slope (slope) was measured as the most steep uprising slope from the first pass, rapid-rising part of time intensity curve. The peak indicated the concentration of contrast material in the intravascular and extravascular interstitial space and represented as the tissue perfusion of bone marrow. The slope was most influenced by the MVD within the tissue and

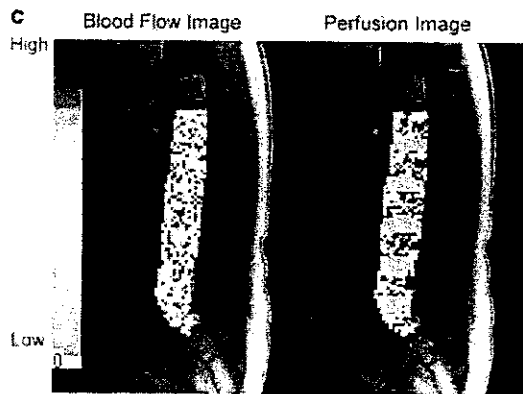
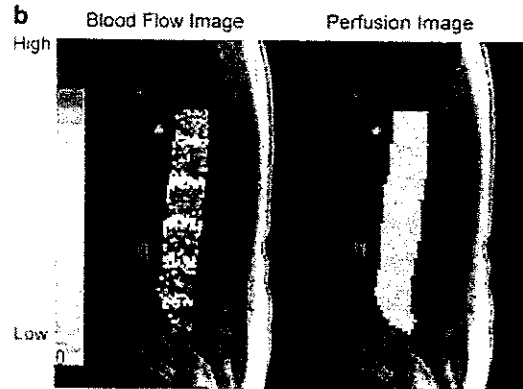
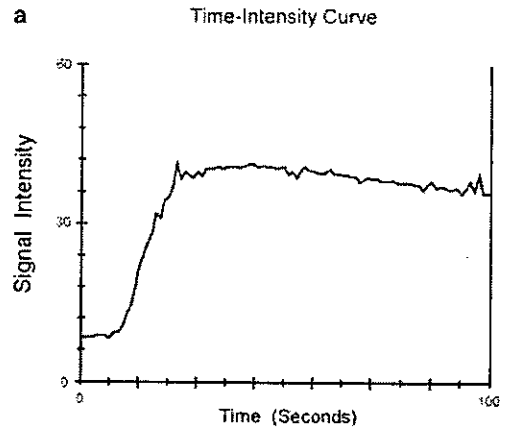


Figure 3 Dynamic magnetic resonance imaging study in a 43-year-old male with newly diagnosed AML. He relapsed after chemotherapy. (a) Time-intensity curve showed rapid, high uprising increment during the first-pass, which indicated high angiogenesis of the bone marrow. (b) Color-coded blood flow (slope) and perfusion (peak) images at early increment phase of the dynamic scanning. (c) Color-coded blood flow (slope) and perfusion (peak) images at mid-equilibrium phase of the dynamic scanning. (b, c) The angiogenesis map of the vertebral bone marrow was automatically displayed from 0 to 100s of the dMRI: the red color represented high angiogenesis, yellow as intermediate and green color as low angiogenesis, shown in the color-coding bar chart.

reflected the blood flow of bone marrow. We measured the peak and slope of vertebral bodies from L1 to L5 of lumbar spine and took the average to represent as the personalized marrow angiogenesis.

For visualization of the angiogenesis map of bone marrow, we developed an easy to use computer program for color-coding map of the dMRI parameters. The computer program uses state-of-the-art information technologies to develop a comprehensive test-bed. Its software architecture has several layers, including an interface layer to visualize images, an analysis layer to compute statistical data, a graphics processing layer to convert image format, and an I/O layer to retrieve/store information. The interface layer uses several subwindows to enable image visualization, show statistical analysis as line charts, and adjust parameters in an auxiliary interface.

Patient characteristics were compared using the Mann-Whitney *U* test. Cut points for high bone marrow blood flow

(slope) or tissue perfusion (peak) group versus low bone marrow blood flow (slope) or tissue perfusion (peak) group of patients were determined by the Classification and Regression Tree (CART) method. CART is a nonparametric regression method that uses the recursive partitioning method to build a decision tree structure and classifies subjects into high- and low groups. Survivals were calculated using the Kaplan-Meier method and compared by the Log-rank test. The data were analyzed using STATISTICA Data Miner software (version 6.0; StatSoft Inc., Tulsa, OK, USA) and MINITAB software (release 13; Minitab Inc., State College, PA, USA).

Bone marrow angiogenesis in AML patients was significantly higher than normal controls as measured by tissue perfusion

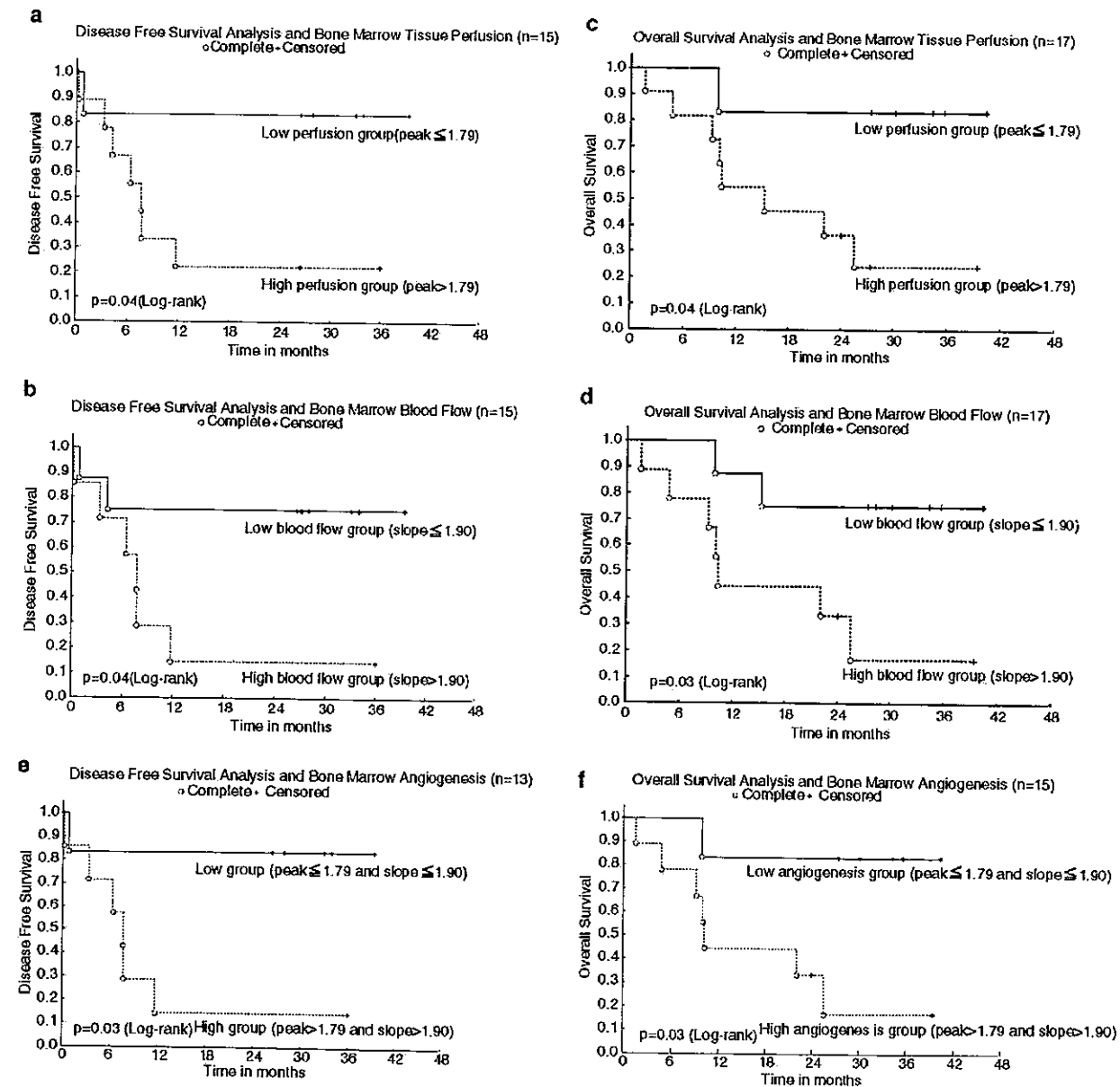


Figure 4 Bone marrow angiogenesis and Kaplan-Meier survival curve of AML patients. Two patients who did not achieve complete remission were also excluded from the disease-free survival analysis. For (e) and (f), the low angiogenesis group was defined as tissue perfusion ≤ 1.79 and blood flow ≤ 1.90 ; high angiogenesis group as tissue perfusion > 1.79 and blood flow > 1.90 . Two patients with either high bone marrow tissue perfusion (peak) or high blood flow (slope), but did not have both high bone marrow blood flow (slope) and high tissue perfusion (peak), were excluded from the analysis.

(peak of AML 2.04 ± 0.69 (mean \pm s.d.) versus peak of control 0.42 ± 0.21) ($P < 0.001$) and blood flow (slope of AML 2.41 ± 1.15 versus slope of control 0.87 ± 0.53) ($P < 0.001$). The time-intensity curve derived from dMRI of lumbar spine was shown in Figure 1a. Color-coded angiogenesis map of bone marrow blood flow and tissue perfusion of one vertebral bone marrow in AML patient and normal control were shown in Figure 1b and c. The dMRI time-intensity curve and color-coded bone marrow blood flow (slope) and tissue perfusion (peak) images in two representative patients were shown in Figures 2 and 3.

The cut-point for high versus low bone marrow tissue perfusion (peak) was set at 1.79 and for blood flow (slope) at 1.90 as determined by the CART analysis. AML patients with high bone marrow tissue perfusion (peak > 1.79) or high blood flow (slope > 1.90) had decreased disease-free survival (DFS) and overall survival (OS) compared to patients with low bone marrow tissue perfusion (peak) or blood flow (slope) as shown in Figure 4a-d. AML patients with high tumor angiogenesis as indicated by both high bone marrow blood flow (slope) and high tissue perfusion (peak) had significantly decreased DFS ($P = 0.03$) and OS ($P = 0.03$) as compared to the patients with low tumor angiogenesis (Figures 4e and f). AML patients (83%) with low tumor angiogenesis remained disease free at 36 months compared to 13% of the patients with high tumor angiogenesis. In total, 83% of AML patients with low tumor angiogenesis remained alive at 40 months compared to 15% of the patients with high tumor angiogenesis.

This is the first report of functional MR imaging of tumor angiogenesis in AML. Our findings that bone marrow angiogenesis is increased in newly diagnosed AML patients and increased bone marrow blood flow and tissue perfusion can predict adverse clinical outcome of AML patients, confirm that angiogenesis may play an important role in the pathogenesis of AML.³

There is increasing evidence that AML may be an angiogenesis-dependent disease with progressive recruitment of blood vessels in the bone marrow.³ Current surrogate markers of angiogenesis can only partially reflect the angiogenesis of hematological malignancies. dMRI may be a better alternative than MVD in bone marrow biopsy specimen because it is noninvasive and can evaluate much bigger bone marrow volumes.⁸ Functional imaging of tumor angiogenesis by dMRI may have a special role in the assessment of bone marrow angiogenesis, predicting the clinical outcome, selection of antiangiogenic therapy or monitoring of response to treatment in AML. dMRI can provide noninvasive, convenient, reproducible serial evaluations of global bone marrow angiogenesis diagnostics with only 100 s' scanning time and total preparation time less than 15 min. A prospective study using repeated dMRI to monitor the tumor angiogenesis before and after treatment in AML patients is currently ongoing in our institution. The real significance of dMRI tumor-angiogenesis parameters as independent prognostic factors in AML or their interaction with other known prognostic factors in AML may need future large clinical investigations.

dMRI measurements of bone marrow blood flow and tissue perfusion, which integrated the total blood vessel density and vasculature functional status (permeability) reported in this study may give a more informative evaluation of global bone marrow angiogenesis in AML. In the bone marrow, the enhancement of contrasts is influenced by concentration of contrast agent in the macrovascular (for example, from paired segmental arteries to intravertebral small arteriole), microvascular (from arterial capillary to sinusoid) factors, and also the extravascular or interstitial compartments. Mainly tissue microvascularization

and perfusion determine the first pass or rapid-rising part (wash-in phase). After the first pass, capillary permeability and interstitial space components contribute to the characteristics of the curve and then yield a further increase, a plateau or an early wash out phase. As shown in the Figures 1a, 2a and 3a, the rapid-rising part or first pass in the time-intensity curve (from the point at SI_{base} to SI_{max}) represented the flushing in of the contrast medium from the arterial capillaries into the extracellular space of the bone marrow cavity within the vertebral body.

The peak enhancement ratio (represents tissue perfusion in this study) has to be regarded as a complex process, including blood inflow, outflow, transit and permeability factors that affect gadolinium concentration at extracellular compartment, reflecting the summation of vessel density and permeability factors. The initial enhancement slope (represents blood flow) was the maximum slope during the initial uprising part of the time-intensity curve and would be most influenced by the MVD within the tissue. The measurements of bone marrow blood flow and perfusion using this dMRI method are practical and reproducible in our previous clinical studies.⁷ For better visualization of the angiogenesis map, we develop a Web-based system, which will enable multiple users to use our tool simultaneously from remote computers. The color image presentation of tumor angiogenesis in AML patients by dMRI is easily interpretable by physicians compared to standard MRI time-intensity curves or data.

In conclusion, bone marrow angiogenesis is increased in AML patients as measured by dMRI. Increased bone marrow angiogenesis can predict adverse clinical outcome in AML. Functional MR imaging of tumor angiogenesis may help to identify the best candidate patients for tailored antiangiogenic therapy and monitor treatment response.

Acknowledgements

We thank Professor Timothy K Shih, Department of Computer Engineering, Tamkang University, Taiwan for the designing of the computer program used for color-coding angiogenesis image.